ESCUELA DE CONSTRUCCIÓN CIVIL
FACULTAD DE INGENIERÍA

Revista de la Construcción
Journal of Construction

Research Article

An alternative approach for increasing the visibility of roads

Serdal Terzi[1], Fatih Ergezer[2*], Mehmet Saltan[3], Sebnem Karahancer[4], Ekinhan Eriskin[5], Ismail Serkan Uncu[6], Oznur Karadag[7], Akay Kurter Kurtman[8], Mehmet Kayakus[9], Kemal Muhammet Erten[10]

1 Department of Civil Engineering, Suleyman Demirel University, Isparta (Turkey), email: serdalterzi@sdu.edu.tr
2 Department of Civil Engineering, Suleyman Demirel University, Isparta (Turkey), email: fatihergezer@sdu.edu.tr
3 Department of Civil Engineering, Suleyman Demirel University, Isparta (Turkey), email: mehmetsaltan@sdu.edu.tr
4 Department of Civil Engineering, Isparta University of Applied Sciences, Isparta (Turkey), sebnem-sargin@isparta.edu.tr
5 Department of Property Protection and Security, Suleyman Demirel University, Isparta (Turkey), ekinhaner-iskin@sdu.edu.tr
6 Department of Electrical and Electronic Engineering, Isparta University of Applied Sciences, Isparta (Turkey), ser-kanuncu@isparta.edu.tr
7 Department of Civil Engineering, Suleyman Demirel University, Isparta (Turkey), oznurkaradag92@gmail.com
8 Rectorate, Alanya Alaattin Keykubat University, Alanya (Turkey), akay.kurtman@alanya.edu.tr
9 Manavgat Faculty of Social and Human Sciences, Akdeniz University, Antalya (Turkey), email: mehmetkaya-kus@akdeniz.edu.tr
10 Department of Building Inspection, Yalvac Technical Sciences Vocational School, Isparta University of Applied Sciences, Isparta (Turkey), email: kemalerten@isparta.edu.tr
*Correspondence: fatihergezer@sdu.edu.tr (F. Ergezer).

Received: 09.03.23; **Accepted:** 12.03.24; **Published:** 31.08.24

Citation: Terzi, S., Ergezer, F., Saltan, M., Karahancer, S., Eriskin, E., Uncu S.I., Karadag, O., Kurtman, A.K., Kayakus, M. and Erten, K.M. (2024). An alternative approach for increasing the visibility of roads. Revista de la Construcción. Journal of Construction, 23(2), 203-217. https://doi.org/10.7764/RDLC.23.2.203

Abstract: Visibility problems occur on highways that are not sufficiently illuminated at night, endangering traffic safety. Phosphor material, which has a natural glow feature under ultraviolet (UV) light, is planned to increase road visibility in areas with inadequate lighting. Phosphor powder (PP) was used in four different percentages (25%, 50%, 75%, and 100%) as fillers in hot mix asphalt (HMA), reduced to filler size. Asphalt specimens were prepared using a super pave gyratory compactor and super pave volumetric mixture design. Compacted specimens were exposed to artificial 12V UV light for 10-minute intervals in a dark room, and UV light absorption was observed. Visibility analyses were performed on the specimens by taking high-resolution photos with long exposure from a distance of approximately 30 cm from the asphalt specimen using a professional camera. According to the analysis results, the visibility values increased by 200.4%, 378.5%, 538.1%, and 728.5% compared to the reference specimen for substitution rates of 25%, 50%, 75%, and 100%, respectively. Experiments were conducted to determine the behavior of the specimens prepared as phosphorus substitutes in the mixture. After selecting the optimum binder contents, the modified Lottman test procedure was applied to measure the specimens' strength values and moisture sensitivity prepared at optimum ratios. The indirect tensile test results show that the 25% PP-substituted specimen had a better strength value. The tensile strength ratio (TSR) value, the ratio of dry and wet tensile stresses, was determined to have minor moisture sensitivity in the 50% PP-substituted specimen. HWTT was applied to the specimen containing 50% PP content, which exhibited the best TSR ratio, resulting in improved rutting performance compared to the reference specimen.

Keywords: Road visibility, phosphor, UV light, image analysis, hot mix asphalt.

1. Introduction

With road construction, it is crucial to illuminate the road structures. Because of traffic safety, roads must be adequately illuminated or visible (Babari et al., 2012; Lin et al., 2023; Erkan et al., 2023). Therefore, improving the visibility of the road is expected to reduce the number of road accidents, especially at night (Assum et al., 1999; Raynham, 2004; Babic et al., 2019; Seidu et al., 2023). Studies have shown that road lighting decreases night accidents by 30%-55% (Leidschendam, 1984; Fisher, 1977; Beyer & Ker, 2009). Moreover, phosphorescent road signs have been determined to reduce fatal accidents by 42.1% at accident hot spots (Yi et al., 2017). It is a common practice to mark road surfaces using gloss materials for increased nighttime visibility on roads (Bi et al., 2020; Burghardt et al., 2021; Villa et al., 2022). While such paints can offer a life of 7-8 months, the service life can be up to 4-5 years with thermoplastic paints (Dormidontovaa & Filatova, 2016). With thermoplastic fluorescent paints on road surfaces under UV light, night vision increased, and vehicle headlights modified with UV light compared to halogen light significantly increased night visibility (Simmons et al., 1997; Turner et al., 1998).

It takes seconds for the human eye to get used to the dark. This process, called dark adaptation, represents the transition from a bright environment to a dark environment. In the sections of the highways with insufficient lighting, glare can be captured for a certain period by utilizing the illumination duration of the phosphor. The minimum time is targeted, taking into account the adaptation period of the human eye to the dark within the luminosity period. The minimum target time was 0.32 mcd/m^2 (Hernandez et al., 2018). The luminance time of the phosphor radiation is also defined as the time for the glare to decrease to 0.32 mcd/m2. It has been observed that the luminous time depends on the characteristics of the phosphor glare capacity (Poelman et al., 2009; Shan et al., 2022). When the studies carried out to increase the visibility of the roads are examined, Ekrias et al. (2009) increase the road visibility by adding some materials to the infrastructure. The effect of aggregate type and color contrast on the lighting performance of the road has been investigated, and light-colored aggregates have a better visibility value than dark aggregates. Another study also confirms that light-colored aggregates in the hot mix asphalt (HMA) increase the visibility of the roads (Ylinen et al., 2011). Alternatively, phosphorous material can be considered for light-colored aggregate. Phosphorous material can glow for a certain period while exposed to UV and purple light (Britannica, 2019).

The use of phosphorus material as a powder in asphalt pavements (Yu et al., 2020; Sheng et al., 2017; Qian et al., 2018; Anwari et al., 2023) and bitumen modification (Filippis et al., 1995; Yu et al., 2020) and in asphalt cement (Voravanicha et al., 2019), there are also some studies on the use of phosphorescent paint mixtures in road marking lines (Lee et al., 2016; Yi et al., 2017; Halefoglu, 2017). The Netherlands N329 highway is the first road to use alumina-based phosphorus compound for road marking purposes (Lyu et al., 2020). Qian et al. (2013) investigated using phosphorous slag as a filler material in HMA. Mechanical properties of HMA with phosphorous slag were determined using laboratory tests. The test results determined that using phosphorous slag as filler material gave a critical resistance to moisture damage in the HMA and increased the resistance of the wheel tracks. Eriskin et al. (2019) studied phosphorous paint to increase the visibility of the HMA. Phosphorous paint was integrated into the mixture in different proportions (15%, 20%, 25%, 30%, 35%, and 40%) based on the weight of the binder. However, Eriskin et al. (2019) studied only phosphorous paint as a mixture additive. The visibility values of the compacted specimens were determined. The main difference in this study is that PP was used as filler material.

The study primarily aims to enhance pavement visibility in road sections with limited or no illumination by utilizing phosphor powder (PP) with natural luminescent properties. Additionally, the mechanical properties provided by different proportions of PP within the mixture are evaluated for asphalt pavements. Therefore, four different substitution rates (25%, 50%, 75%, and 100% by weight of filler material) were used, and each rate's optimum binder content (OBC) was determined. A Superpave volumetric mix design procedure was used to determine the OBC. Specimens were prepared and compacted using a super pave gyratory compactor (SGC) in a 100 mm mold with optimum binder contents. Compacted specimens were exposed to artificial 12 V UV light for 10–minute intervals in a dark room, and UV light absorption was observed. Visibility analyses were performed using a self-written image analysis program on the specimens by taking high-resolution photos with long exposure from a distance of approximately 30 cm from the asphalt specimen using a professional camera. Then, the

strength values of the specimens were obtained, and the TSR values were calculated. Subsequently, the Hamburg wheel tracking test (HWTT) was conducted to determine the rutting performance of the mixture.

The paper is arranged as follows. Section 2 is dedicated to materials (aggregate, bitumen, and PP). The physical, chemical, and morphological properties of the materials (energy dispersive spectroscopy (EDS) and scanning electron microscopy (SEM)) are given in this section. Section 3, under the title of experimental studies, mixture design, image analysis, modified Lottman test, HWTT, and findings are given. The summary and conclusions are given in the last section.

2. Materials and methods

2.1. *Materials*

2.1.1. Aggregate

The aggregates used in the study are limestone aggregates obtained from the asphalt construction site of Isparta. To determine the physical properties of the full, tests were applied for coarse, delicate, and filler materials. The results are shown in Table 1.

Table 1. Properties of the limestone aggregate.

Aggregate size	Specification	Unit	Standard	Value
Coarse aggregate	Specific gravity	g/cm^3	ASTM C 127	2.72
	Water absorption	%	ASTM C 128	2.74
	Abrasion	%	TS EN 1097-1	19.2
Fine aggregate	Specific gravity	g/cm^3	ASTM C 127	2.68
	Water absorption	%	ASTM C 128	0.155
Filler	Specific gravity	g/cm^3	ASTM C 854	2.62

2.1.2. Bitumen

Bitumen with a penetration value of 50-70 is used in the study and is obtained from the asphalt construction site of Isparta Municipality in Turkey. Traditional bitumen tests such as softening point, penetration, ductility, and specific gravity tests are applied to determine the properties of base bitumen. In order to determine the performance class of bitumen, rotational viscometer (RV), rotational thin film oven test (RTFOT), pressure aging vessel (PAV), dynamic shear rheometer (DSR), beam bending rheometer (BBR) tests are applied according to Superpave design criteria. Bitumen test results are given in Table 2. Bitumen performance grade (PG) has been determined as 64-22.

Table 2. Properties of the bitumen.

Specification	Unit	Value	Limit value	Standard
Penetration @25 °C	0.1 mm	61.2	50-70	ASTM D5
Softening point Ring&Ball	°C	49.8	46-54	ASTM D36
Ductility @25°C, 5 cm/dk	cm	>100	>100	ASTM D113
Specific gravity, g/cm^3	g/cm^3	1.029		ASTM D70
Rotational viscosity @135 °C, ≤3Pa.s	Pa.s	0.000475		ASTM D4402
Rotational viscosity @165 °C	Pa.s	0.00015		ASTM D4402
DSR G*/sinδ>1 kPa @10 rad/s (Failure temperature)	°C	66.8		ASTM D7552
DSR G*/sinδ>1 kPa @10 rad/s (Grade)	°C	64		ASTM D7552
Mass loss	%	0	< 0.5	
Permanent penetration	%	72.3	≥ 50	ASTM D5
Softening point change	°C	+3.5	≤ 9	ASTM D36
DSR G*/sinδ>2.2 kPa @10 rad/s (Failure temperature)	°C	66.2		ASTM D7552
DSR G*/sinδ>2.2 kPa @10 rad/s (Grade)	°C	64		ASTM D7552
DSR G*.sinδ<5.000 kPa @10 rad/s (Failure temperature)	°C	28.6		ASTM D7552
DSR G*.sinδ<5.000 kPa @10 rad/s (Grade)	°C	22		ASTM D7552
BBR S≤300 MPa, m≥0.300 @60 s (Grade)	°C	-12		ASTM D6648
BBR S≤300 MPa, m≥0.300 @60 s (m-value)		0.325	≥ 0.3	ASTM D6648
BBR S≤300 MPa, m≥0.300 @60 s (Stiffness)	MPa	213	≤ 300	ASTM D6648
Performance grade (PG) 64-22				

2.1.3. Phosphorous powder (PP)

Phosphorous powder (PP), used in the study, is provided as pigments. PP is used as filler material by sieving through the No.200 sieve. The specific gravity of PP used in the study is determined as 1,407 g/cm^3. Figure 1. shows the appearance of PP under sunlight (left) and a dark ambiance after being left under sunlight for one minute (right).

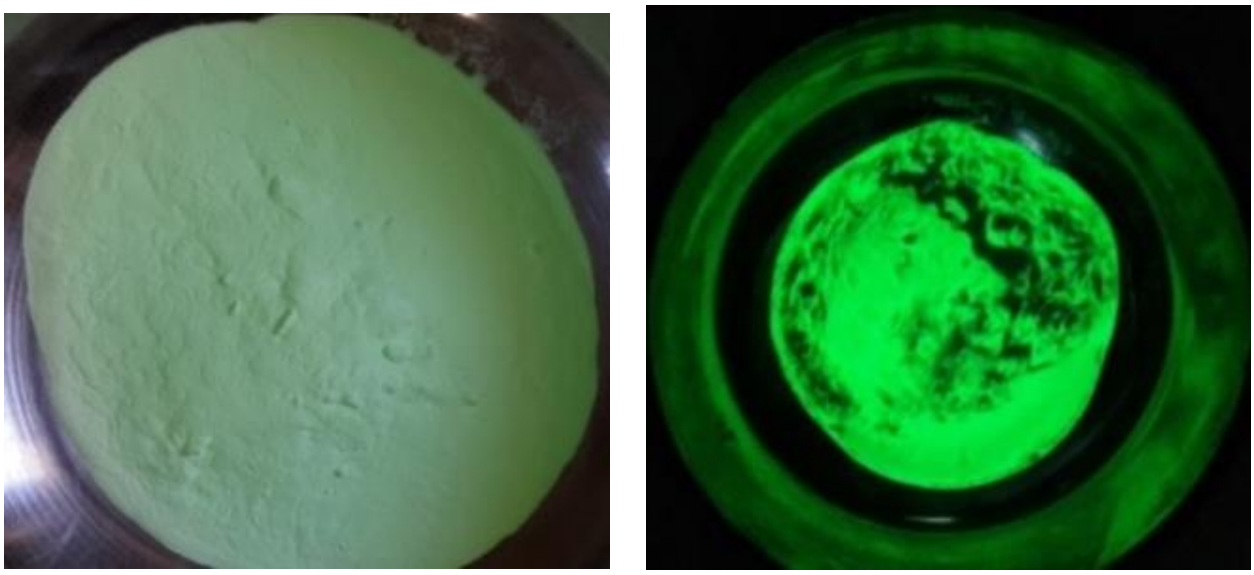

Figure 1. PP under sunlight (left) and in the darkroom after leaving under sunlight for one minute (right).

SEM-EDS analyses are applied to limestone, and PP materials are used as fillers. According to SEM-EDS analysis, the surface conditions of the materials, the components they contain, and their percentage distributions are determined. SEM images of limestone and PP are given in Figures 2 and 3. PP EDS analysis is given in Figure 4. The chemical composition of PP is given in Table 3.

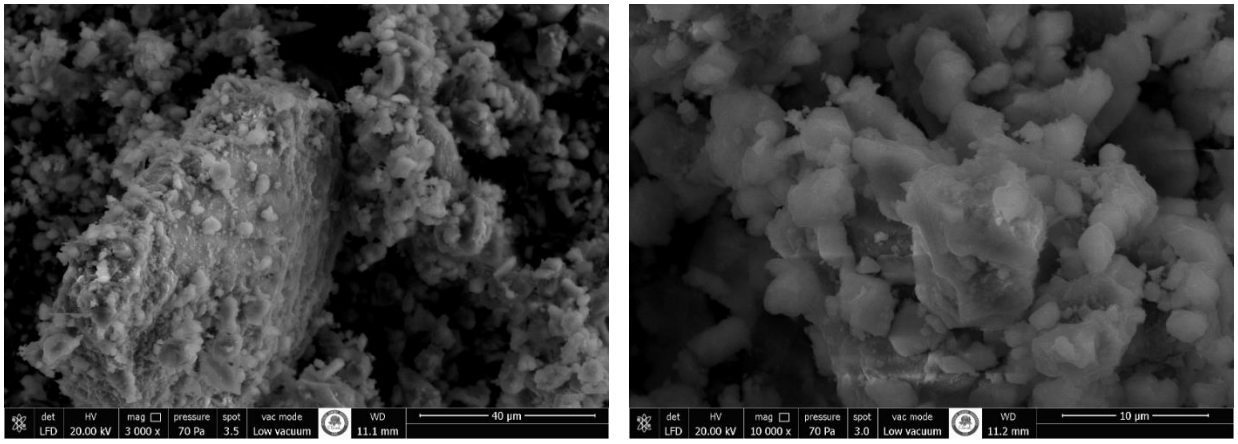

Figure 2. SEM images of limestone filler.

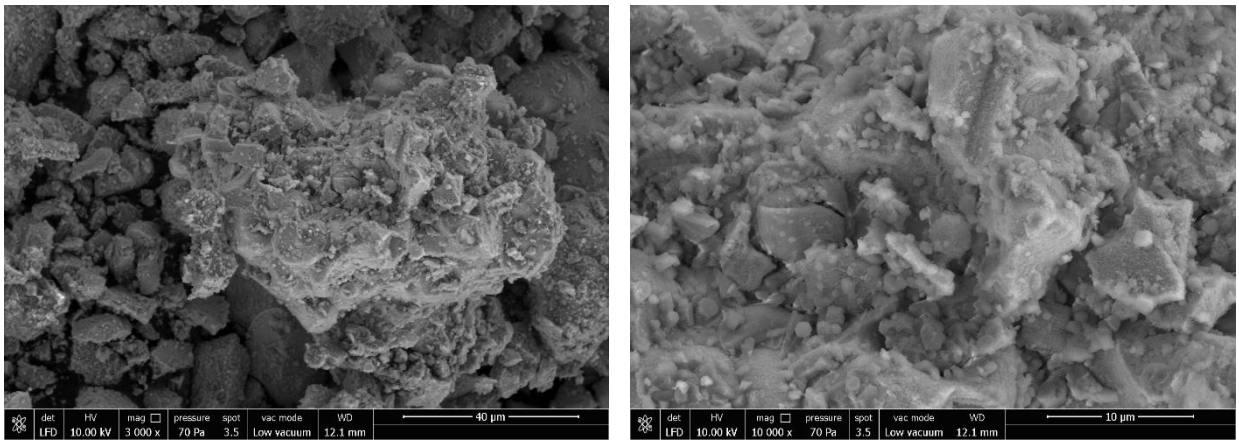

Figure 3. SEM images of PP.

When examining the SEM images, results for Figures 2 and 3 are provided in conglomerates ranging from 10 to 40 mm. In the limestone aggregate SEM images, a smoother structure is observed at 10 mm, while the PP material appears to have a more granular structure. Overall, when looking at the SEM images, it can be seen that the materials exhibit approximately the same topographic structure.

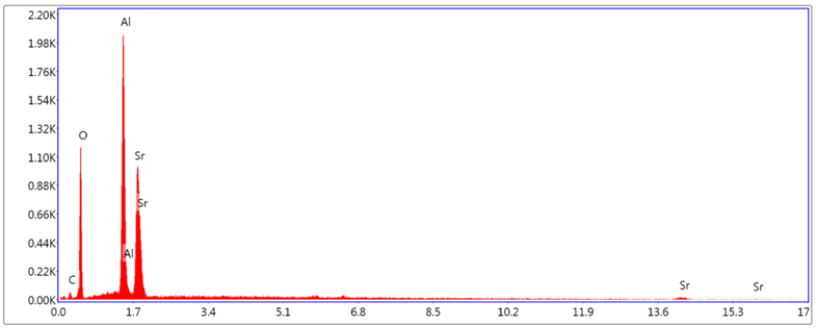

Figure 4. EDS analysis of PP.

Table 3. Chemical composition of PP.

Element	C	O	Al	Sr	Eu
Weight (%)	6.37	42.39	23.41	25.29	2.54

The EDS analysis reveals that the PP material comprises carbon (C), oxygen (O), aluminum (Al), strontium (Sr), and europium (Eu) elements. Among these, Sr and Eu are known to influence the phosphorescent glow time, while Al_2O_3 acts as an activator. According to the EDS analysis, the substitution of Al has increased the phosphor's luminescence time (Nance & Spark, 2020). The general chemical formula is represented as SrAl2O4:Eu2+.

3. Experimental results and analysis

3.1. Volumetric mix design

The Superpave volumetric mix design method determined the mixture's OBC and aggregate gradation. This design aims to increase the performance of HMA against fatigue, aging, and wheel tracking (Cominsky et al., 1994). The gradation curve is shown in Figure 5.

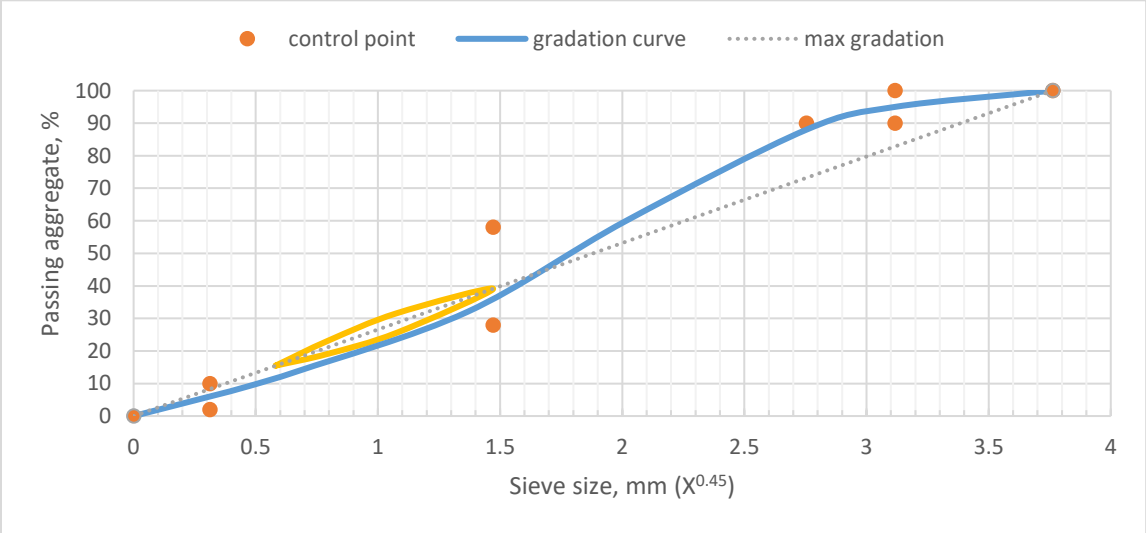

Figure 5. Superpave gradation curve.

The super pave gradation curve contains control points and restricted zone areas. Aggregate gradation should be designed to pass through the control points while avoiding the restricted zone. The control points are placed at three points, which are the selected nominal maximum aggregate size, an intermediate sieve (2.36 mm), and the smallest sieve size (0.075 mm) (Mampearachchi & Fernando, 2012). The restricted zone is the region between 2.36 mm and 0.3 mm. The presence of sand or fine-grained materials characterizes this zone.

The specimens are prepared in four different binder content (4%, 4.5%, 5%, 5.5%) by compacting with 125 gyrations (NDEs) using the super pave gyratory compactor (SGC) to determine the OBC of the mixtures. The bitumen content, which gives 4% air void, is predetermined as optimum bitumen content and checked whether the content rate ensures the VMA and VFA specification limits. The change in the PP substitution rate and bitumen content is shown in Figure 6.

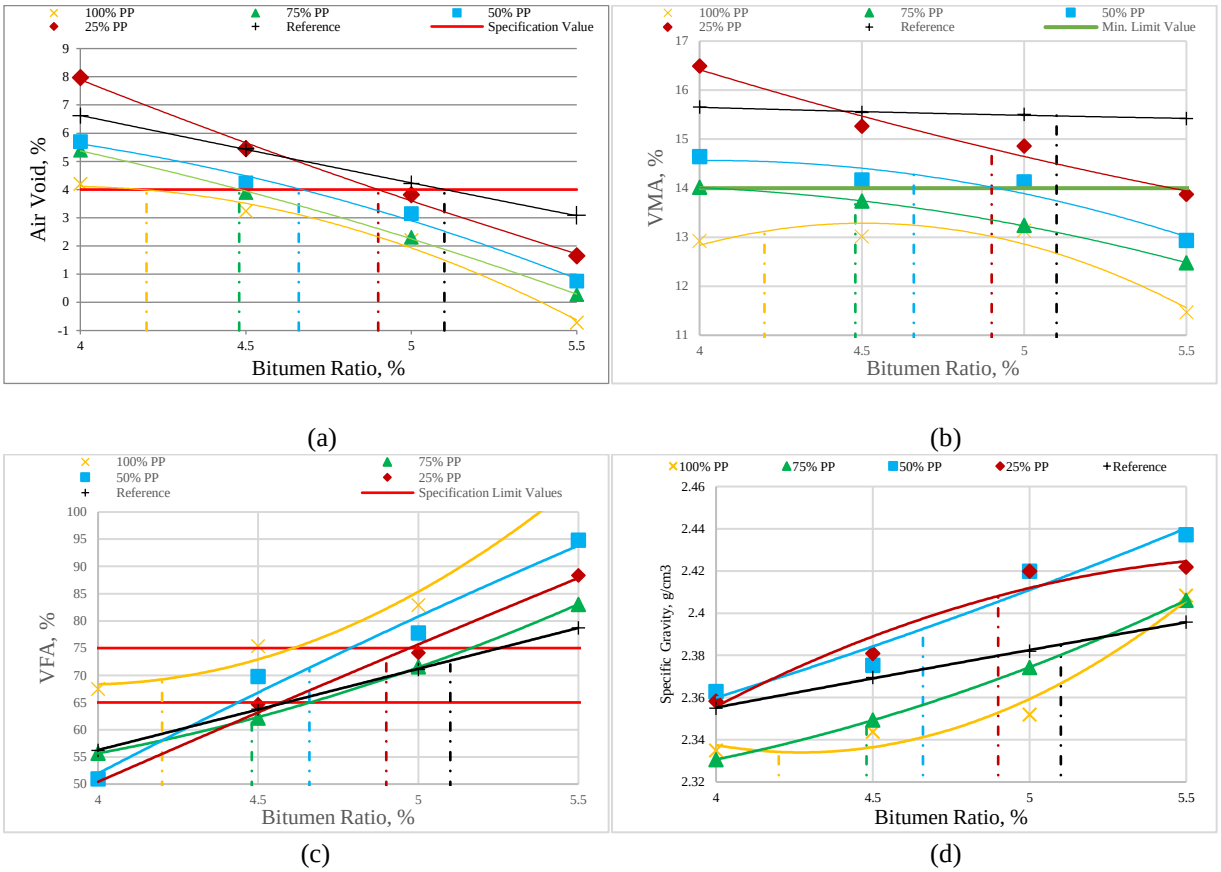

Figure 6. (a) Air void for reference, and each different substituted specimen, (b) VMA values for reference and each different substituted specimen, (c) VFA values for reference and each different substituted specimen, (d) Specific gravity values for reference and each different substituted specimen.

As seen in Figure 6a, the OBC of the specimens is 5.1%, 4.90%, 4.62%, 4.48%, and 4.2% for reference, 25%, 50%, 75%, and 100% PP substituted specimens, respectively. As seen in Figure 6b, specimens prepared at 75% and 100% PP substitution rates according to VMA results were valued outside the specification limit ranges. Figure 6c shows that the specimen prepared at a 75% PP substitution rate according to VFA results is valued outside the specification limit ranges. The change in specific gravity values is shown in Figure 6d.

3.2. Image analysis

Image processing is an increasingly widespread method with the development of technology. Image processing is an essential function for distinguishing, identifying, and measuring gray-scale and color images, and it is used in many scientific and technological areas. The lenses used in image acquisition devices are defined as CCD, and the images from these sensors are divided into three different color levels. These colors are represented by red, green, and blue (RGB). Each pixel in a black-and-white image (1 bit) takes a value of 0-1, whereas, in a gray-scale image (8 bits), each pixel has image density values ranging from 0 to 255. The RGB images comprise 24-bit image density values, each with 8 bits for red, green, and blue color channels (Mendoza & Lu, 2015).

For the visibility analysis in this study, high-resolution photographs are taken on the reference, and 25%, 50%, 75%, and 100% PP substituted specimens with a professional camera at 10-minute intervals, aiming to saturate the PP-replaced specimens with UV light under 12V UV light in a dark room. Figure 7 shows the views of the specimens under UV light.

The photos are transferred to an algorithm to analyze the images taken in this study, where each image pixel is digitized and converted to RGB colors. Then, the analysis area is selected, and the pixels are converted to a grayscale using Equation 1 (Eriskin et al., 2019).

$$Gray = \frac{R+G+B}{3} \qquad (1)$$

when the image is grayed out, the pixels have a value between 0 to 255. To correct the defects caused by the light source, filter the shining regions on the image with the help of Equation 2 (Eriskin et al., 2019).

$$\sum_{n=1}^{TA} x = \begin{cases} x = 0, & P_{gray} < F_{min} \\ x = 1, & F_{min} < P_{gray} < F_{max} \\ x = 0, & F_{max} < P_{gray} \end{cases} \qquad (2)$$

TA is the total area of the selected region. Filtered images are converted to black (0) and white (255). The visibility ratio is determined by dividing the visible pixel counts after filtering to the total pixel counts in the selected area. According to the visibility analysis, the visibility rates increase with increasing PP content (Figure 8).

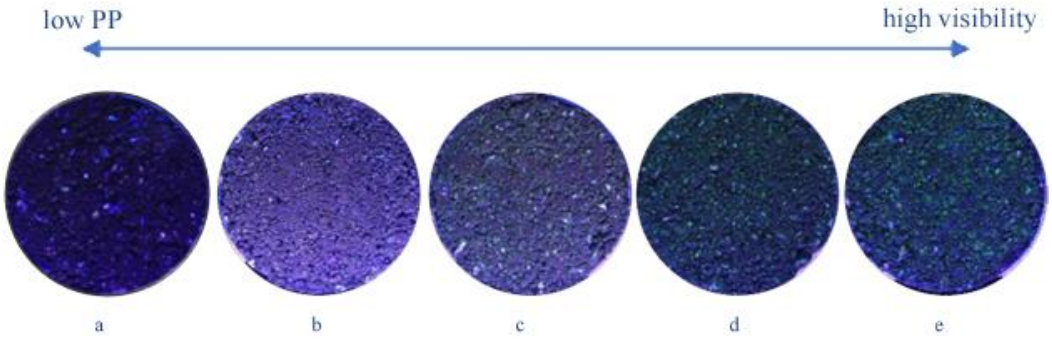

Figure 7. (a) The view of the reference (a) and 25% (b), 50% (c), 75% (d), and 100% (e) substituted specimens under UV light.

As seen in Figure 7, it is observed that the visible areas on the sample expanded with the increase in the PP additive percentage. Whereas the dark areas on the reference sample occupied a larger area, the augmentation in PP content resulted in the dispersion of UV light-sensitive pigments across the sample, enhancing visibility.

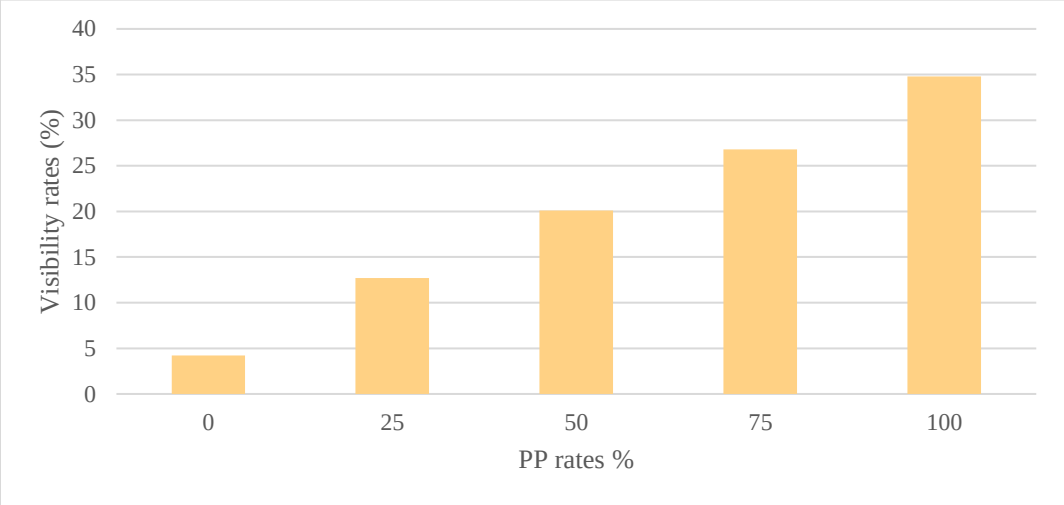

Figure 8. Visibility rates for each different substituted specimen.

As seen in Figure 8, the visibility rates in 25%, 50%, 75%, and 100% PP substituted specimens are 12.7%, 20.1%, 26.8%, and 34.8%, respectively. After obtaining the visibility rates, the increase in visibility is compared with the reference specimen. It is determined that the 25%, 50%, 75%, and 100% PP substituted specimens are 200.4%, 378.5%, 538.1%, and 728.5% more visible than the reference specimens.

The elements constituting phosphors' properties play a significant role in luminescence. Several atomic structures become excited during luminescence, initiating the phosphorescent emission (Shionoya et al., 2018). The study included visibility measurements on specimens containing PP, revealing that the specimens maintained their glare levels for an average of 30 minutes. Subsequently, a decrease in their illumination is observed. It is noted that the glow time varied depending on the type of phosphorus, typically ranging from 5 minutes to 24 hours (Hernandez et al., 2018).

3.3. Modified Lottman test

The modified Lottman test is conducted to determine the strength values of the specimens following the AASHTO T-283 standard. According to AASHTO T-283 test procedures, at least six specimens are compacted using the SGC device. After the compaction of the specimens, they are divided into two groups (IDTunconditioned and IDTconditioned). All the specimens are cured for 72 hours at 40˚C. After the curing process, unconditioned specimens are kept at ambient temperature until the conditioned specimens are. Conversely, the conditioned specimens are soaked in the water bath for 24 hours at 25°C. After 24 hours, the specimens are vacuum-saturated until the saturation level reaches 55-80% intervals and placed in an excellent cabin for 16 hours at -18˚C. After freezing the specimens, they are soaked in the water bath for 24 hours at 60°C for thawing. Last, the specimens are soaked for 2 hours at a 25°C water bath and loaded till failure with the unconditioned specimens. The ratio of the conditioned to unconditioned specimen's strength value gives the tensile strength ratio where the moisture susceptibility of the specimens is obtained. The indirect tensile (IDT) strength and tensile strength ratio (TSR) values are shown in Figure 9. The indirect tensile test (IDT) is utilized to assess the strength values of the specimens. IDT formulas should be given as follows:

$$IDT = \frac{2*P}{\pi*t*D} \quad (3)$$

where IDT is tensile strength value (kPa); P is the maximum load (kN); t is specimen thickness (m); D is the diameter of the specimen (m).

Once the fracture values of IDTwet and IDTdry specimens are acquired, the TSR value can be calculated, as Do et al. (2021) outlined. The TSR value must meet or exceed 80% per the specification requirements. Calculate the TSR as follows:

$$TSR = \frac{IDT_{wet}}{IDT_{dry}} \quad (4)$$

where TSR is tensile strength ratio (%); IDTwet represents the strength value (kPa) of the conditioned specimens; IDTdry represents the strength value (kPa) of the unconditioned specimens.

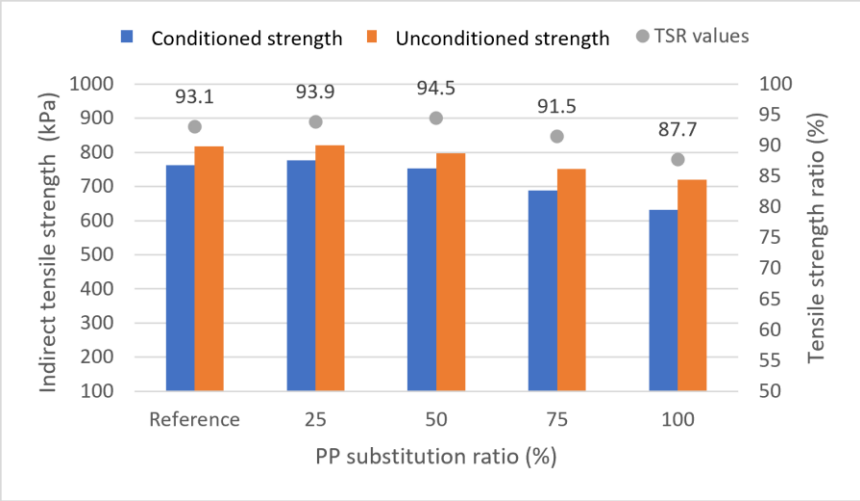

Figure 9. IDT and TSR of the specimens.

As seen in Figure 9, both conditioned and unconditioned IDT strength values of the specimens containing 25% PP are higher than the reference specimen. Other specimen results are less than the reference specimen. When the TSR ratios given in Figure 9 are examined, it has been seen that the TSR value of all specimens is higher than the specification limit value of 80%. TSR values of the mixtures prepared in 25% and 50% PP substitution rates are higher than the TSR of the reference specimen. It is seen that the TSR reached a peak value in the mixture prepared at a 50% PP substitution rate and then decreased. The lowest TSR value is in the mixture prepared with 100% PP substitution content. As the sensitivity to moisture is tested with the TSR value, the sensitivity of all specimens to moisture is higher than the specification limit value.

3.4. Hamburg wheel tracking test

The Hamburg wheel tracking test (HWTT) is standardized according to AASHTO T-324. HWTT is a widely used method to determine the resistance to tracking and moisture sensitivity of HMA. HWTT allows us to perform a minimized simulation of the actual field conditions in the laboratory, allowing us to determine the wheel tracking resistance and moisture sensitivities of asphalt mixtures (Tsai et al., 2016). Two specimens, each with a diameter of 150 mm and a height of 63.5 mm, are prepared using SGC. The test is conducted with a water temperature set at 50°C. Steel wheels utilized in the experiment are 204 mm in diameter and 47 mm in width. A load of 703 N is applied to each specimen employing steel cylindrical wheels. The test continues until reaching a maximum of 20000 passes or a 12.5 mm wheel tracking in the center of the specimen. The device stops once either of these conditions is met, and the test concludes (Izzo & Tahmoressi, 1999; Han & Shiwakoti, 2016). As a result, it gives the wheel tracking value as a graph according to the number of passes.

The HWTT test is applied to the specimens containing 50% PP content and the reference sample, which exhibited a peak TSR value. The specimen with 50% PP content outperformed the reference specimen in rut depth. The 50% PP specimen demonstrated superior moisture sensitivity and better rutting performance than the reference sample. The graph of the reference 50% PP substituted showed specimens in Figure 10.

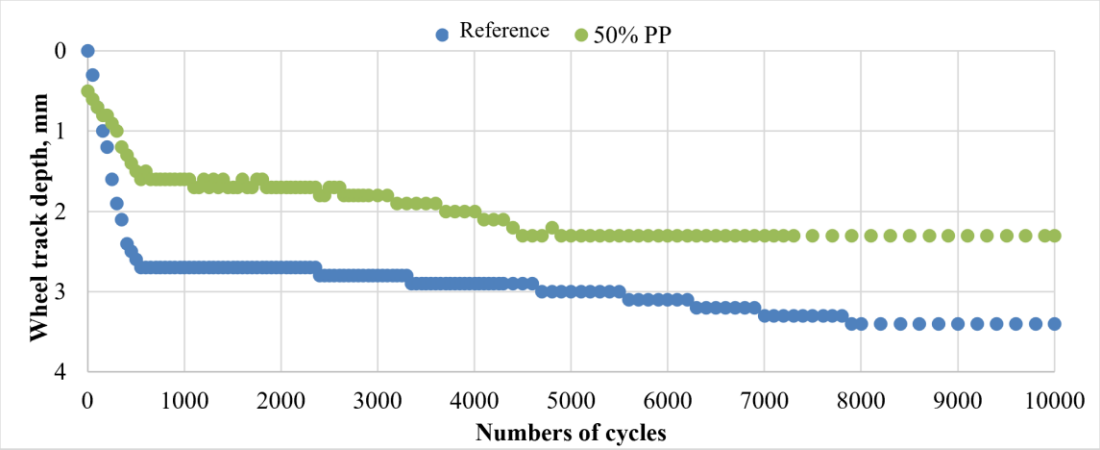

Figure 10. HWTT graph for reference and 50% PP substituted specimens.

As seen from Figure. 10, HWTT results of the reference specimen and %50 PP substitute specimens provided specification values. The specimen containing 50% PP found a minor wheel-tracking depth.

4. Summary and comments

This study used PP material as a filler substitute in HMA. OBC was determined by preparing the gradation according to the Superpave volumetric mixture design. Visibility analysis, IDT, moisture susceptibility, and HWTT were applied. The obtained values and recommendations are summarized as follows.

1. The gradation was prepared within the study according to the super pave volumetric mixture design. PP was substituted into the mixture in 25%, 50%, 75%, and 100% of the filler contents. OBC in each combination was determined. Optimum bitumen rates were 5.1%, 4.90%, 4.62%, 4.48%, and 4.2% for the reference and 25%, 50%, 75%, and 100% PP substituted specimens. As the PP ratio increases, the optimum amount of bitumen decreases up to 17.6%. This situation is an economic advantage because it leads to less use of bitumen.

2. Visibility analysis was performed on the specimens prepared with different PP substitution contents. High-resolution photographs taken in a dark room under UV light were analyzed using a visibility analysis algorithm. According to the image results, the analysis determined that the visibility values increased as the PP content increased to 728.5%. According to these results, using PP would cause a severe increase in pavement visibility.

3. After obtaining the strength test results, 25% of the PP-substituted specimens gave 0.3% better unconditioned and 1.8% better-conditioned strength values than the reference specimen. However, increasing the PP substitution rate gradually decreases strength values. For the calculated TSR, it was observed that 50% of the PP-substituted specimen gave the highest value, with an improvement of 1.5%. However, increasing the PP rate worsens the TSR value compared to the reference specimen. The HWTT was conducted using the sample with the highest TSR ratio, which contained 50% PP content. The reference and specimen with 50% PP content met the test standards. Remarkably, the specimen with 50% PP content exhibited a 30% improvement in rutting performance compared to the reference specimen.

4. Based on a comprehensive analysis considering bitumen content, visibility results, IDT strength, TSR values, and HWTT results, it can be concluded that the optimal PP substitution content is 50%. This conclusion is supported by several factors: the 50% PP content leads to lower bitumen content (compared to 75% and 100% PP content), a higher visibility ratio, the highest TSR value, and reduced rutting depth. Therefore, 50% PP content emerges as the most favorable option across multiple performance indicators.

Using PP on the pavement will significantly increase visibility, contributing considerably to road traffic safety, especially in unlit areas at night. The phosphor visibility level is observed to be maintained for 30 minutes on average in the observations. It will profoundly contribute to road visibility, especially in areas with insufficient lighting and intense traffic accidents. In future studies, the phosphorus contribution could be subjected to the Semi-Circular Bending test (SCB) under low and medium temperature conditions. Additionally, its effect on visibility could be tested on a real-scale road section, with plans to evaluate it under different UV spectra.

Author contributions: **Serdal Terzi:** Conceptualization, Writing-editing, Supervision. **Fatih Ergezer:** Conceptualization**,** Methodology, Investigation, Writing-review, Visulization. **Mehmet Saltan:** Conceptualization, Writing-editing, Supervision. **Sebnem Karahancer:** Methodology, Investigation, Writing-review, Visulization. **Ekinhan Eriskin:** Methodology, Investigation, Writing-review, Visulization, Writing-editing. **Ismail Serkan Uncu:** Conceptualization, Writing-editing, Supervision. **Oznur Karadag:** Investigation, Visulization, Methodology. **Akay Kurter Kurtman:** Visulization, Writing-review, Conceptualization. **Mehmet Kayakus:** Conceptualization, Visulization, Investigation. **Kemal Muhammet Erten:** Methodology, Visulization, Investigation

Funding: We thank the Scientific and Technological Research Council of Turkey (TUBITAK) for supporting the study with grant number 217M478.

Conflicts of interest: There is no conflict.

References

Anwari, R. A., Coskun, S., & Saltan, M. (2023). Research on recycle of waste fluorescent lamp glasses and use as mineral filler in asphalt mixture. Journal of Material Cycles and Waste Management, 25(1), 258-271. https://doi.org/10.1007/s10163-022-01525-3

Assum, T., Bjornskau, T. Fosser, S. & Sagberg, F. (1999). Risk Compensation- the Case of Road Lighting. Accident Analysis and Prevention, 31(5), 545-553. https://doi.org/10.1016/S0001-4575(99)00011-1

Babari, R., Hautiere, N. Dumont, E. Paparoditis, N. & Misener, J. (2012). Visibility Monitoring Using Conventional Roadside Cameras – Emerging Applications. Transportation Research Part C: Emerging Technologies, 22, 17-28. https://doi.org/10.1016/j.trc.2011.11.012

Babic, D., Scukanec, A., Babic, D., & Fiolic, M. (2019). Model for predicting road markings service life. The Baltic Journal of Road and Bridge Engineering, 14(3), 341-359. https://doi.org/10.7250/bjrbe.2019-14.447

Beyer, F. R., & Ker, K. (2009). Street lighting for preventing road traffic injuries. Cochrane database of systematic reviews, (1).

Bi, Y., Pei, J., Chen, Z., Zhang, L., Li, R., & Hu, D. (2021). Preparation and characterization of luminescent road-marking paint. International Journal of Pavement Research and Technology, 14(2), 252-258. https://doi.org/10.1007/s42947-020-0229-3

Britannica., (2019). Phosphor. Date of Access: 17.01.2019. https://www.britannica.com/science/phosphor

Burghardt, T. E., Pashkevich, A., & Bartusiak, J. (2021). Solution for a two-year renewal cycle of structured road markings. Roads and Bridges-Drogi i Mosty, 20(1), 5-18.

Cominsky, R, J., Huber, G, A. Kennedy, T, W. & Anderson, M. (1994). The Superpave Mix Design Manuel for New Construction and Overlays. SHRP-A-407, National Research Council, Washington DC.

Do, T. C., Lee, H. J., Baek, C. M., & Nguyen, T. T. (2021). Mechanical characteristics of shear strength ratio used for moisture susceptibility evaluation of asphalt mixtures. International Journal of Pavement Engineering, 22(4), 447-454. https://doi.org/10.1080/10298436.2019.1614586

Dormidontova, T. V., & Filatova, A. V. (2016). Research of influence of quality of materials on a road marking of highways. Procedia Engineering, 153, 933-937. https://doi.org/10.1016/j.proeng.2016.08.256

Ekrias, A., Eloholma, M. & Halonen, L. (2009). The Effects of Colour Contrast and Pavement Aggregate Type on Road Lighting Performance. Light and Engineering, 17(3), 76-91.

Erişkin, E., Karahançer, Ş. Terzi, S. Saltan, M. Çapalı, B. Uncu, İ.S. & Çoskunsu, S. (2019). Increasing the Visibility of Roads Using Phosphorous Paint. Road Materials and Pavement Design, 20(1), 199-210. https://doi.org/10.1080/14680629.2017.1374999

Erkan, A., Hoffmann, D., Kreb, N., Vitkov, T., Kunst, K., Peier, M. A., & Khanh, T. Q. (2023). Required Visibility Level for Reliable Object Detection during Nighttime Road Traffic in Non-Urban Areas. Applied Sciences, 13(5), 2964. https://doi.org/10.3390/app13052964

Filippis, P.D., Giavarini, C. & Scarsella, M. (1995). Improving the Aging Resistance of Straight-Run Bitumens by Addition of Phosphorous Compounds. Elsevier Science, 74(6), 836-841. https://doi.org/10.1016/0016-2361(95)00015-W

Fisher, A.J. (1977). Road Lighting as an Accident Counter-Measure. Australian Road Research Board ARRB, 7(4), 3-16.
Halefoğlu, Y. Z. (2017). Investigation of the Usability of Lanthanide Element Doped Long-lasting CaAl2O4 Phosphorescent Pigment as a Traffic Road Marking Line, Çukurova University Journal of the Faculty of Engineering and Architecture, 32(4), 121-126. https://doi.org/10.21605/cukurovaummfd.383190

Han, J., and Shiwakoti, H. (2016). Wheel Tracking Methods to Evaluate Moisture Sensitivity of Hot-Mix Asphalt Mixtures. Frontiers of Structural and Civil Engineering, 10(1), 30-43. https://doi.org/10.1007/s11709-016-0318-1

Izzo, R, P., and Tahmoressi, M. (1999). Use of Hamburg Wheel-Tracking Device for Evaluating Moisture Susceptibility of Hot-Mix Asphalt. Transportation Research Record, 1681(1), 76-85. https://doi.org/10.3141/1681-10

Lee, Y. M., Kim, S. T., Jeong, W. S., & Kim, H. R. (2016). Night Visibility Evaluation of Phosphorescent Road Line Markings. International Journal of Highway Engineering, 18(4), 69-75.

Leidschendam, S., (1984). Visibility Aspects of Road Lighting. SWOV Institute for Road Safety Research, 12.

Lin, H., Chen, F., & Zhang, H. (2023). Active luminous road markings: A comprehensive review of technologies, materials, and challenges. Construction and Building Materials, 363, 129811. https://doi.org/10.1016/j.conbuildmat.2022.129811

Lyu, L., Chen, Y., Yu, L., Li, R., Zhang, L., & Pei, J. (2020). The Improvement of Moisture Resistance and Organic Compatibility of SrAl2O4: Eu2+, Dy3+ Persistent Phosphors Coated with Silica–Polymer Hybrid Shell. Materials, 13(2), 426. https://doi.org/10.3390/ma13020426

Mampearachchi, W, F., Fernando, P, R, D. (2012). Evaluation of The Effect of Superpave Aggregate Gradations on Marshall Mix Design Parameters of Wearing Course. Journal of The National Science Foundation Sri Lanka, 40(3), 183-194.

Mendoza, F., & Lu, R. (2015). Basics of Image Analysis. Hyperspectral Imaging Technology in Food and Agriculture, Food Engineering Series, Springer, New York, NY.

Nance, J., & Sparks, T. D. (2020). Comparison of coatings for SrAl2O4: Eu2+, Dy3+ powder in waterborne road striping paint under wet conditions. Progress in Organic Coatings, 144, 105637. https://doi.org/10.1016/j.porgcoat.2020.105637

Poelman, D., Avci, N., & Smet, P. F. (2009). Measured luminance and visual appearance of multi-color persistent phosphors. Optics express, 17(1), 358-364.

Qian, G., Bai, S. Ju, S. & Huang, T. (2013). Laboratory Evaluation on Recycling Waste Phosphorus Slag as the Mineral Filler in Hot-Mix Asphalt. Journal of Materials in Civil Engineering, 25(7), 846-850. https://doi.org/10.1061/(ASCE)MT.1943-5533.0000770

Qian, G., Wang, K. Bai, X. Xiao, T. Jin, D. & Huang, Q. (2018). Effects of Surface Modified Phosphate Slag Powder on Performance of Asphalt and Asphalt Mixture. Construction and Building Materials, 158, 1081-1089. https://doi.org/10.1016/j.conbuildmat.2017.09.123

Raynham, P. (2004). An Examination of the Fundamentals of Road Lighting for Pedestrians and Drivers. Lighting Research and Technology, 36(4), 307-316. https://doi.org/10.1191/1365782804li125oa

Rojas-Hernandez, R. E., Rubio-Marcos, F., Rodriguez, M. A., & Fernandez, J. F. (2018). Long lasting phosphors: SrAl2O4: Eu, Dy as the most studied material. Renewable and Sustainable Energy Reviews, 81, 2759-2770. https://doi.org/10.1016/j.rser.2017.06.081

Seidu, R. K., Sun, L., & Jiang, S. (2023). A systematic review on retro-reflective clothing for night-time visibility and safety. The Journal of the Textile Institute, 1-13. https://doi.org/10.1080/00405000.2023.2212194

Shan, B., Yang, X., Cao, X., Deng, M., & Tang, B. (2022). Preparation of high-luminescent materials and application of luminescent coatings in road engineering. Journal of Materials in Civil Engineering, 34(8), 04022159. https://doi.org/10.1061/(ASCE)MT.1943-5533.0004305

Sheng, Y., Zhang, B. Yan, Y. Chen, H. Xiong, R. & Geng, J. (2017). Effects of Phosphorous Slag Powder and Polyester Fiber on Performance Characteristics of Asphalt Binders and Resultant Mixtures. Construction and Building Materials, 141, 289-295. https://doi.org/10.1016/j.conbuildmat.2017.02.141

Shionoya, S., Yen, W. M., & Yamamoto, H. (Eds.). (2018). Phosphor handbook. CRC press.

Simmons, C., Mahach, K., Knoblauch, D., Nitzburg, M., Tignor, S., & Wochinger, K. (1997, October). Field evaluation of ultraviolet (uv)-activated fluorescent roadway delineation. In Proceedings of the Human Factors and Ergonomics Society Annual Meeting (Vol. 41, No. 2, pp. 1392-1392). Sage CA: Los Angeles, CA: SAGE Publications. https://doi.org/10.1177/107118139704100219 2

Tsai, B. W., Coleri, E., Harvey, J. T., & Monismith, C. L. (2016). Evaluation of AASHTO T 324 hamburg-wheel track device test. Construction and Building Materials, 114, 248-260. https://doi.org/10.1016/j.conbuildmat.2016.03.171

Turner, D., Nitzburg, & M. Kloblauch, R. (1998). Ultraviolet Headlamp Technology for Nighttime Enhancement of Roadway Markings and Pedestrians. Transportation Research Record Journal of Transportation Research Board, 1636(1), 124-131. https://doi.org/10.3141/1636-20

Villa, C., Brémond, R., Eymond, F., & Saint-Jacques, E. (2022). Characterization of luminescent road markings. Lighting Research & Technology, 14771535221111052. https://doi.org/10.1177/14771535221111052

Voravanicha, K., Leelachao, S., Sahasithiwat, S., Kumnorkaew, P., & Dangtungee, R. (2019). Natural rubber filled with phosphorescent materials for pavement. Materials Today: Proceedings, 17, 1971-1976. https://doi.org/10.1016/j.matpr.2019.06.244

Yi, Y., Lee, K., Kim, S., & Choi, K. (2017). Effectiveness Analysis and Application of Phosphorescent Pavement Markings for Improving Visibility. KSCE Journal of Civil and Environmental Engineering Research, 37(5), 815-825.

Ylinen, A.M., Pellinen, T. Valtonen, J. Puolakka, M. & Halonen, L. (2011). Investigation of Pavement Light Reflection Characteristics. Road Materials and Pavement Design, 12(3), 587-614. https://doi.org/10.1080/14680629.2011.9695262

Yu, H., Li, S., Qian, G., Gong, X., & Wang, K. (2020). Experiment evaluation on the surface treatment of phosphorus slag (PS) micro powder for asphalt modification. Construction and Building Materials, 262, 119931. https://doi.org/10.1016/j.conbuildmat.2020.119931

Yu, H., Zhu, X., Qian, G., Gong, X., & Nie, X. (2020). Evaluation of phosphorus slag (PS) content and particle size on the performance modification effect of asphalt. Construction and Building Materials, 256, 119334. https://doi.org/10.1016/j.conbuildmat.2020.119334

Copyright (c) 2024. Terzi, S., Ergezer, F., Saltan, M., Karahancer, S., Eriskin, E., Uncu S.I., Karadag, O., Kurtman, A.K., Kayakus, M. and Erten, K.M. This work is licensed under a Creative Commons Attribution-Noncommercial-No Derivatives 4.0 International License.